Fast Approximate Symmetry Plane Computation as a Density Peak of Candidates

Alex König[a] and Libor Váša[b]
Dept. of Computer Science and Engineering, University of West Bohemia, Pilsen, Czech Republic

Keywords: Symmetry Detection, Reflection Symmetry, Symmetry Plane, Density Peak Computation.

Abstract: Symmetry is a common characteristic exhibited by both natural and man-made objects. This property can be used in various applications in computer vision and computer graphics. There are various types of symmetries, amongst the most prominent belong reflection symmetries and rotation symmetries. In this paper, a method focusing on the fast detection of approximate reflection symmetry of a 3D point cloud with respect to a plane is proposed. The method is based on the creation of a set of candidates that are represented as rigid transformations, and have assigned weights, reflecting the estimated quality of the candidate. The final symmetry plane corresponds to a density peak in the transformation space. The method is demonstrated to be able to find symmetry planes in various objects in 3D, with its main benefit being the speed of the computation.

1 INTRODUCTION

In mathematics, an object is called *symmetric*, if a transformation that maps the object back onto itself exists. In other words, the object is invariant under certain classes of transformations. The class of the transformations the object is invariant under defines the type of symmetry. The most common types are *reflection*, *rotation* and *translation symmetry*. Symmetry can be defined for objects represented by images, point clouds, meshes or volumetric data.

If an object remains exactly the same after applying the symmetry transformation it is *perfectly symmetric*. As this rarely occurs in natural shapes, it makes sense to define *approximate symmetry*. In that case the defined transformation does not map the object onto itself exactly. To quantify how strong the approximate symmetry is, a similarity measure is needed. If only part of the object is symmetric, it is *partially symmetric*. This means that only parts of the object are invariant under certain classes of transformations. Partial symmetry can again be perfect or approximate. Objects that do not posses any of the above mentioned characteristics are labeled as *asymmetric*.

Reflection symmetry of an object is, in 2D, defined by a line, and in 3D, by a plane. The object or its parts are reflected onto the other side of the line or the plane onto the other matching object or part. Rotational symmetry is defined by an angle and a point in 2D or a line in 3D. The object or its parts are rotated by the given angle around the given point or line. Translation symmetry is defined by a direction and a distance. The object or its parts are moved by the given distance in the defined direction.

Detecting symmetry is an active topic in computer vision and computer graphics. Symmetry detection can be used in various applications, such as data compression, model denoising and symmetrization, shape reconstruction, model synthesis, object recognition and classification (Mitra et al., 2013).

The proposed method focuses on the fast detection of approximate reflection symmetries in point clouds and polygon meshes, primarily in 3D, but could be extended to work in lower, or higher dimensions. The main advantage of this method is its low computation time and ability to work with various types of input. The user can tune the parameters of the method and influence the accuracy of the output symmetry, with the trade off of slightly higher computation time.

Our algorithm uses the RANSAC scheme. First creating a set of symmetry plane candidates, then filtering out the candidates of lower quality. The symmetry plane is determined by finding a density peak in the transformation space, using a clustering algorithm or density estimation at each candidate location, which is faster. Both approaches require specifying

[a] https://orcid.org/0000-0002-2680-8345
[b] https://orcid.org/0000-0002-0213-3769

König, A. and Váša, L.
Fast Approximate Symmetry Plane Computation as a Density Peak of Candidates.
DOI: 10.5220/0013119200003912

In *Proceedings of the 20th International Joint Conference on Computer Vision, Imaging and Computer Graphics Theory and Applications (VISIGRAPP 2025) - Volume 1: GRAPP, HUCAPP and IVAPP*, pages 185-192
ISBN: 978-989-758-728-3; ISSN: 2184-4321

a metric in the transformation space. Such a metric was defined by Hruda et al. (Hruda et al., 2019).

The rest of this paper is structured as follows: the related work is reviewed in Section 2, describing other methods of the detection of reflection symmetries in 3D objects. Section 3 elaborates on symmetry and the measuring of symmetry. Section 4 introduces the proposed algorithm. In Sections 5, 6, 7 and 8 the steps of the algorithm are explained in more detail, followed by the results in Section 9, where the method is evaluated on triangle meshes in 3D.

2 RELATED WORK

Many methods have been proposed for the detection of symmetry of objects using various approaches. Some methods use neural networks to find the reflection symmetry plane in an input object. Gao et al. (Gao et al., 2021) formulate the symmetry detection problem as a per point classification problem, calculate the initial guess and then use optimization to refine the symmetry plane. Ji and Liu (Ji and Liu, 2019) first convert the input shape to voxels and train an unsupervised 3D convolution neural network to extract the plane of symmetry. However, while those methods are fast, they require a training dataset to set up the neural network, and the performance of the second mentioned method deteriorates significantly with higher resolution of the voxels.

Another group of symmetry detection methods exploits the visual properties of symmetry. These methods first generate a set of images of the object from various angles. In the method by Gothandaraman et al. (Gothandaraman et al., 2020) a rather small set of generated images is processed to find the rotation or the reflection symmetry. Li et al. (Li et al., 2016) define viewport entropy, expressing how much information each generated image holds. Symmetry of this entropy distribution then corresponds to the symmetry of the object. However, this method only detects symmetry planes that pass through, or near, the center of the bounding sphere of the input object.

Other methods are based on the geometry of the input object. Given the input is a mesh, the methods mainly work with the location of the vertices, and some of them require the information about the connectivity to compute a neighborhood of any given vertex. These methods are diverse in their approaches. Cicconet et al. (Cicconet et al., 2017) reflect the original dataset with respect to an arbitrary plane, then register it onto the original, and use the reflection and registration mappings to derive the symmetry plane. Such an approach could run into problems as registration sometimes does not work well on symmetric objects. The method by Martinet et al. (Martinet et al., 2006) uses generalized moment functions, whose extremes define the symmetry planes. Nagar and Raman (Nagar and Raman, 2019) define the problem of detecting approximate reflection symmetry as a linear assignment problem between the input points, and determine the symmetry by solving an optimization problem on a smooth Riemannian product manifold. Other methods rely on a RANSAC scheme. They first generate a set of candidate symmetry planes that is filtered to select a smaller subset, which will be further processed to obtain the final reflection symmetry plane. For example, Ecins et al. (Ecins et al., 2017) use a non-linear optimization of the plane parameters, and Hruda et al. (Hruda et al., 2021) define a differentiable symmetry measure that allows using gradient based optimization. Mitra et al. (Mitra et al., 2006) use clustering to find the most often reoccurring symmetry plane. However, with the use of clustering the question arises how to select the best cluster and how to select the best candidate within this cluster.

3 REFLECTION SYMMETRY

While there are multiple types of symmetry, this work primarily focuses on approximate reflection symmetry in 3D, represented by a plane. Two points p_1 and p_2 are symmetric, if the following equation holds:

$$p_2 = r(\sigma, p_1) = p_1 - 2d\vec{n} \tag{1}$$

The function $r(\sigma, p_1)$ is the function reflecting point p_1 over plane σ, and it can be expressed using the distance d of the point p_1 from the plane σ, and the normal vector of the plane $\vec{n}$ oriented towards the half-space with the point p_1. That means, point p_2 is a projection of p_1 to the other side of the plane.

An object represented by a point cloud P or a polygon mesh whose shape can be well represented by its set of vertices P, $P = \{p_i, i = 1, ..., n\}$, is symmetric if, for some plane σ, the points can be organized into pairs satisfying the Equation (1). In other words, every point from P reflects onto another point from P.

Symmetry is often not perfect, especially for real-world objects. For approximate symmetry we test if the point p_1 reflects not exactly onto the point p_2, but into its close vicinity. For an object to be approximately symmetric with respect to a plane, we can count how many points are approximately symmetric, and test if the percentage of such points is higher than a given threshold. For the purposes of this paper, the term "symmetry" will refer to approximate reflection symmetry with respect to a plane.

3.1 Symmetry Measure

To measure the strength of approximate symmetry of an object, a function that evaluates the quality of a symmetry plane can be defined. If the value given by this function is higher than a defined threshold, the object is deemed as symmetric.

As the function measuring the symmetry of the object we use the metric proposed by Hruda et al. (Hruda et al., 2021). For an object represented by a point cloud $P = \{p_i, i = 1,...,n\}$, $p_i = (x_i, y_i, z_i)$, this metric can be expressed as follows:

$$sym(\sigma) = \sum_{i=1}^{n}\sum_{j=1}^{n}\phi(||r(\sigma, p_i) - p_j||). \qquad (2)$$

The symmetry plane is denoted σ and $\phi(l)$ is a Wendland's function (Wendland, 1995) as modified by Hruda et al. (Hruda et al., 2021), where its value decreases to 0 as its parameter l increases. The higher the value of $sym(\sigma)$ is, the more symmetric the object is with respect to the plane σ.

A relative symmetry measure can be defined as:

$$sym_{rel}(\sigma) = \frac{\sum_{i=1}^{n}\sum_{j=1}^{n}\phi(||r(\sigma, p_i) - p_j||)}{\sum_{i=1}^{n}\sum_{j=1}^{n}\phi(||p_i - p_j||)}. \qquad (3)$$

The higher the value, the more symmetric the object is with respect to a plane σ. If an object is perfectly symmetric with respect to a plane σ_s with points far from one another in space, then $\phi(||p_i - p_j||)$ is zero unless $p_i = p_j$, and $\phi(||r(\sigma_S, p_i) - p_j||)$ is zero unless $r(\sigma_s, p_i) = p_j$. The value of $sym_{rel}(\sigma_s)$ for this object is 1, which is the best achievable score. If the same object is asymmetric with respect to a plane σ_a then $\phi(||r(\sigma_s, p_i) - p_j||)$ is always zero, and the value of $sym_{rel}(\sigma_s)$ is also 0.

If a different object with points closer to one another is perfectly symmetric with respect to a plane σ_t, then $\phi(||p_i - p_j||)$ is a non-zero value for all points p_j in the neighborhood of p_i, and $\phi(||r(\sigma_t, p_i) - p_j||)$ is a non-zero value for all points p_j in the neighborhood of $r(\sigma_t, p_i)$. Since all points p_i always reflect onto another point of the object, the value of $sym_{rel}(\sigma_t)$ for such object is also 1.

3.2 Symmetry Transformation as A matrix

The symmetry transformation from Equation (1) can be represented using a 4×4 transformation matrix T:

$$r(\sigma, p) = Tp. \qquad (4)$$

The matrix T represents the reflection with respect to any general plane in space σ described as

$$\sigma = ax + by + cz + d, \qquad (5)$$

where (x, y, z) are the coordinates of points in the plane. The normal of the plane can be written as $n = (a, b, c)$, and the parameter d represents the distance of the plane from the origin.

To reflect a point p with respect to the plane σ, it is also possible to shift both the plane and the point in such a way that the plane passes through the origin, then apply the reflection around this transformed plane, and finally move the reflected point back. The matrix T can therefore be written as

$$T = M_t M_{r0} M_{\text{-}t}, \qquad (6)$$

where the translation to the origin is described as a 4×4 translation matrix $M_{\text{-}t}$ and the translation back as a matrix M_t. The reflection around the plane passing through the origin is described as a 4×4 matrix M_{r0} with the following form (Kovács, 2012):

$$M_{r0} = \begin{bmatrix} 1-2a^2 & -2ab & -2ac & 0 \\ -2ab & 1-2b^2 & -2bc & 0 \\ -2ac & -2bc & 1-2c^2 & 0 \\ 0 & 0 & 0 & 1 \end{bmatrix}. \qquad (7)$$

4 ALGORITHM OVERVIEW

Let us present an outline of the proposed method to compute the approximate symmetry plane. The details of the individual steps are in the next Sections.

The input of the algorithm is a set of points P representing an object, where $P = \{p_i, i = 1,...,n\}$, $p_i = (x_i, y_i, z_i)$, and the output is its approximate symmetry plane. The steps of the algorithm are: input point cloud simplification, candidates creation, candidates filtering and candidate space analysis and density peak computation.

In the first step the input point cloud P is simplified to a lower number of points. Then the candidates for the symmetry plane are generated. Due to the approach to the generation, the candidates are evaluated, to verify if they represent viable symmetries.

The candidates are generated in such a way that, if the same plane is generated multiple times, it likely represents the plane of symmetry of that object. For approximately symmetric objects no two generated planes might be the same, but some generated planes will be similar. As each candidate plane can be represented by a transformation matrix, a density function can be computed in the transformation space. The most prominent symmetry plane is located at the density peak, and is deemed the approximate plane of reflection symmetry of the input point cloud P.

5 POINT CLOUD SIMPLIFICATION

The number of the points in the input point cloud is reduced to accelerate the computation. A simplified point cloud still represents the original shape well enough, even with a rather low number of points, if an appropriate simplification method is used, as concluded by Hruda et al. (Hruda et al., 2021).

Down-sampling the input point cloud randomly could create a point set that does not represent the shape of the original object very well. To sample the point cloud regularly, and so the details are not completely omitted, all of the points from the input point cloud $P = \{p_i, i = 1, ..., n\}$, are inserted into a 3D grid, and for each cell the average point is computed. These points then form the simplified point cloud. The simplification is performed iteratively, while increasing the size of the cells, until the resulting point count reaches the desired number of points m.

Using this algorithm, two simplified versions of the input point cloud are created, point cloud $P_1 = \{p_i, i = 1, ..., m\}$, and point cloud $P_2 = \{p_i, i = 1, ..., k\}$, where $m > k$. The default values are set to $m = 1000$ and $k = 100$.

6 CANDIDATES CREATION

The second step is to create candidate symmetry planes that sample the transformation domain. As ideal symmetry plane reflects each point from the point cloud onto some other point from the point cloud, a set of candidate planes can be created by taking all possible pairs of points from the input point cloud and for each pair creating a plane that reflects these two points onto each other. As it can be too computationally expensive to work with all the candidate planes the input points P generate, we work with the simplified point cloud P_1 in this step.

For each unique point pair $p_i p_j$, where $p_i, p_j \in P_1$, a perfect symmetry plane is created. This plane reflects p_i onto p_j and passes through the midpoint of the line connecting p_i and p_j. The midpoint p_m and the plane normal n can be computed as follows:

$$p_m = (p_i + p_j)/2, \tag{8}$$

$$n = \frac{p_j - p_i}{||p_j - p_i||}. \tag{9}$$

7 CANDIDATES FILTERING

Some of the created candidate planes reflect only few points from P_1 onto each other, and skew the results of the density peak computation. So, the set of generated candidates is filtered to remove those invalid planes, increasing the algorithm speed and accuracy.

For each plane a *least common point set* (LCP) between the points of the object and the points of its reflection can be created. If the number of points in that set is higher than a given threshold t_a, then the plane provides viable symmetry. The value of t_a influences how strict the filtering will be. The higher the threshold value is, the more points have to be symmetric with respect to the plane, for the plane to pass the test. To speed up the filtering step, a simplified point cloud can be used. Our experiments show that it is sufficient to use the point cloud P_2 with 100 points.

To further accelerate the pruning of the candidates, similar planes are grouped together and evaluated at the same time. As a representative of the group serves an average plane computed from all the planes in the group, which is then tested against the LCP requirement. Since only similar planes will be grouped together, if the average plane is not a viable symmetry, the planes it represents also were not viable symmetries, and can be discarded. The number of planes in such groups should be small in most cases, and, removing them will not negatively influence the density peak computation. If the number of planes in such a group is higher, removing them will prevent from identifying high density at a point in the transformation space that does not correspond to a viable symmetry plane. To separate the candidate planes into groups, a 4D grid data structure is used. The grid is described in more detail in Section 7.1.

7.1 Plane Grid

To divide the candidate planes into groups, where all planes in a group are similar, a 4D grid can be used. A plane can be represented by Equation (5). The plane's indices in a 4D grid can then be computed as:

$$\begin{aligned} i &= \lfloor a/s_{cell} \rfloor, \\ j &= \lfloor b/s_{cell} \rfloor, \\ k &= \lfloor c/s_{cell} \rfloor, \\ l &= \lfloor d/(r \cdot s_{cell}) \rfloor, \end{aligned} \tag{10}$$

where r is the radius of the point cloud computed as the mean distance of points from their centroid, and s_{cell} is a user parameter specifying the size of the grid cell, with value from the interval $(0, 1]$.

7.2 Filtering Algorithm

On the input of the filtering algorithm there are the created candidate planes, and an acceptance threshold t_a. The average distance of any two points in P_2 is computed and denoted $avgD$. The algorithm uses a counter variable lcp. The steps of the filtering algorithm are described below:

1. Add all created planes into a plane grid.
2. For each cell in the grid:
   - Create an average plane σ_{avg} from all planes in that cell.
   - Set $lcp = 0$.
   - For each point p_j from P_2:
   (a) Compute its reflection $p_r = r(\sigma_{avg}, p_j)$.
   (b) Find the closest point p_{jc} to p_r, $p_{jc} \in P_2$.
   (c) Compute the distance d of p_{jc} and p_r. If $d < avgD/10$, then the point p_r is considered a reflection of p_j, and lcp is incremented.
   - If $lcp < t_a$, then the plane σ_{avg} is not a symmetry plane. All of the planes in that cell will not be further considered as candidates.

8 CANDIDATE SPACE ANALYSIS

As stated in Section 4, in the generated set of candidates, there should be many transformations close to the optimal symmetry transformation. This higher number of candidates in a small area forms a density peak in the space of the transformations that must be located. A density peak can be found by estimating the density at each candidate location as described in Section 8.1. For this, the relations between two candidates need to be expressed and the amount of (dis)similarity between them must be computed. The used metric is described in Section 8.2.

8.1 Density Peak Computation

As explained in Section 3.2, a reflection with respect to a plane is given by a matrix T as in Equation (6).

Given an input set of symmetry transformation matrices $\mathcal{T} = \{T_i, i = 1, ..., k\}$, a density estimation function ρ can be defined in the transformation space. The density peak can be found as a transform T^* where $\rho(T^*) > \rho(T_i)$ for any i. The density function is expressed in the following equation:

$$\begin{aligned}\rho(T_k) &= \sum_i w_i K(d(T_i, T_k)) \\ &= \sum_i w_i e^{-Dd(T_i,T_k)^2/r},\end{aligned} \tag{11}$$

where the density is computed for the transformation candidate T_k, T_i are the other transformation candidates in the set $\mathcal{T}$, w_i is the weight of T_i, which can further modify its influence, and $d(T_i, T_k)$ is the distance of T_k from T_i that will be described in more detail in Section 8.2. To sample the density estimation function a kernel function K is used. Here K is a simple Gaussian, where D is the spread parameter and r is the radius of the points computed as the mean distance of points from point cloud centroid.

The weights w_i are used because in the transformation space there can be multiple points with high density. Those can either be secondary symmetry planes, or planes that do not create any significant symmetry, but were not filtered out in the third step of the algorithm. To avoid those false peaks, the weights w_i are set as the value of symmetry measure computed using the Equation (2). As this value indicates how close the candidate plane is to a perfect symmetry plane, viable symmetry planes will have higher weights and will influence the resulting density more.

If the set of candidates is too large to compute a sum over all candidates T_i, the fact that the candidate transforms that are far from T_k do not significantly contribute to the overall density can be exploited. Given the spread parameter D and some small threshold t, only samples within a radius $d_r = r\sqrt{-ln(t)}/D$ contribute more than t to the overall density value. The task is to find for each evaluated T_k a set of candidates up to the distance d_r. To achieve this task, the Vantage Point Tree (VPT) (Yianilos, 1993) can be used. VPT is a binary tree, where all the left children of any given node contain values that are closer to the value in the parent than a given threshold, and all the right children contain values that are farther.

To speed up the computation of the weights w_i, a similar approach as in the filtering step is adopted. The candidate planes are inserted into a plane grid, the weight is computed for each average plane, and set to all planes in the cell.

The algorithm can be modified to find multiple most prominent symmetries. A threshold d_t would need to be defined, specifying the distance of density peaks in the candidate space, for them to be considered different symmetry planes. Then k density peaks can be found as transforms T_1^*, T_2^*, ..., T_k^*, where each two transforms are further from each other than d_t and $\rho(T_1^*) \geq \rho(T_2^*) \geq ... \geq \rho(T_k^*) > rho(T_i)$.

8.2 Distance Metric in Candidate Space

To find the density peak, a metric describing the distance between candidates is needed. A candidate can be represented by a matrix T, see Equation (6).

As reflection is a rigid transformation, it can be decomposed into translation and reflection. The metric has to relate these different degrees of freedom and the size of the mesh. For larger meshes, a small rotation of the symmetry plane has bigger effect on the resulting reflection, and the object could get misaligned.

Therefore, instead of comparing the transformations, the difference of their effect on the input data can be compared. This approach is an extension of a metric defined by Hruda et al. (Hruda et al., 2019), where the squared distance between two transformations T_1 and T_2 can be written as follows:

$$\begin{aligned} d(T_1,T_2)^2 &= \sum_{i=1}^{n} ||T_1(p_i) - T_2(p_i)||^2 \\ &= 2\sum_{i=1}^{n} p_i^T p_i + nt_1^T t_2 + nt_2^T t_2 \\ &\quad -2diag(R_1^T R_2) \cdot diag(\sum_{i=1}^{n} p_i p_i^T). \end{aligned} \tag{12}$$

The parameters p_i are the points of the object, R_1 is the reflection part and t_1 is the translation part of the transformation T_1, R_2 is the reflection part and t_2 is the translation part of the transformation T_2.

This metric can be used after the input object's orientation and translation is normalized. The object is translated, so the condition $\sum_{i=1}^{n} p_i = 0$ is satisfied, and rotated, so the matrix $\sum_{i=1}^{n} p_i p_i^T$ is diagonal.

This metric is relatively fast to compute, as the scalar value $\sum_{i=1}^{n} p_i^T p_i$ and vector $diag(\sum_{i=1}^{n} p_i p_i^T)$ can be pre-computed for the given input point cloud. To make the metric independent on the size of the point cloud, it can be divided by its radius r.

9 RESULTS

The proposed method was implemented using *C#* and ran on computer with CPU *Intel(R) Core(TM) i7-9700K*, 32 GB of memory and *Windows 10* operating system. The method was tested on input meshes with various point counts, acquired from public repositories (Fang et al., 2008; Jacobson, 2024; Levoy et al., 2005; Shilane et al., 2004), and the results were compared with the method by (Hruda et al., 2021), which outperforms other methods in terms of robustness, accuracy and speed. Both methods use the same symmetry measure. The results were evaluated using the relative symmetry measure from Equation (3), and the execution time measured in milliseconds.

As can be seen in Table 1, our density based method has three parameters. The parameter *acceptance threshold* t_a, and the *plane grid cell size* s_{cell} are both given as a number between 0 and 1, and are used during the candidate filtering. The last parameter, the *spread parameter* D, is used during the density peak computation. The exact values of the parameters usually do not change the resulting plane by much. The values in Table 1 are chosen empirically.

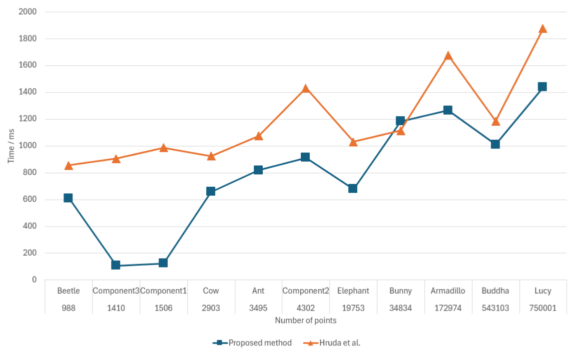

Figure 1: Graph representing the relationship between the computation time in milliseconds and the number of points of a model for our method and the Hruda et al. method (Hruda et al., 2021).

The most vital steps of our algorithm are the candidate filtering and the use of groups of similar planes during the weight computation in the candidate space analysis step, as they influence the speed of the algorithm the most. So it is important to choose the right values of t_a and s_{cell}. The exact speedup depends on how the candidates sample the candidate space, which in turn depends on the distribution of the input points.

The parameter t_a affects the size of the LCP needed to accept the plane as viable symmetry plane, and its value can be set closer to 1 if a strong symmetry is expected in the input and closer to 0 if weak symmetry is expected. The higher the value, the fewer candidates are considered for the density peak computation, and the faster the algorithm is.

The parameter s_{cell} influences how many groups of candidates are created, and how many weights w_i are computed. Lower values often lead to better symmetry planes, and higher values mean less groups are created and the algorithm is faster. The recommended value of s_{cell} is 0.1, and it can be lowered if the algorithm does not return a viable symmetry plane.

Our method is faster than the Hruda et al. method, with the exception of the *Bunny* model, see Figure 1. For the *Bunny* model a strong symmetry cannot be expected due to the positions of the head and the body of the bunny, so the value of parameter t_a has to be lower. Combined with the low value of s_{cell}, it means there is a higher number of created candidates, sorted into a higher number of groups. All of this negatively influences the computation time and our method ends up being slower than the Hruda et al. method.

The higher the value of the relative symmetry

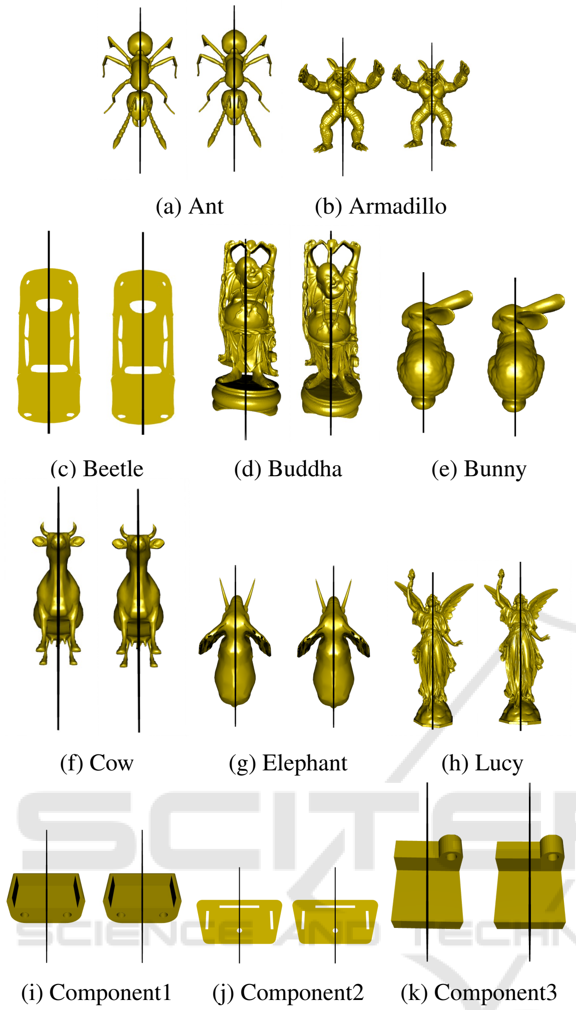

(a) Ant (b) Armadillo

(c) Beetle (d) Buddha (e) Bunny

(f) Cow (g) Elephant (h) Lucy

(i) Component1 (j) Component2 (k) Component3

Figure 2: Resulting symmetry planes for Table 1, left: symmetry plane by our method, right: the symmetry plane by the Hruda et al. method (Hruda et al., 2021).

measure sym_{rel}, the more symmetric the object is with respect to the given plane. Since the planes acquired using our method return smaller values of sym_{rel}, they are of worse quality than those computed by Hruda et al. method. If the resulting planes are examined visually, they do not significantly differ from each other. The results can be seen in Figure 2, with symmetry planes found by our method on the left, and the planes found by Hruda et al. method on the right.

For the *Beetle* model there is a noticeable difference in results if the parameter t_a is set to lower value. This result can be seen in Figure 3. The model has two strong symmetries, for the horizontal plane, the value of the symmetry measure is smaller, but the generated symmetry candidates lie closer to each other. This is caused by the distribution of the input points. If the parameter is set higher, to $t_a = 0.6$, the horizontal planes are filtered out, and do not skew the results.

These results demonstrate the importance of the filtering step. Similarly, to limit such cases, the weights in the density computation step are computed.

Our method also works well for models with sparser point sampling, such as the models *Component1*, *Component2* and *Component3*, where the points of the mesh are situated near the corners and holes, with long edges between them. Our method can also find prominent approximate symmetry planes, such as for the *Bunny* model, where the body is symmetric with respect to one plane and the head with respect to another, or the *Lucy* model.

To accelerate, our method exploits the similarities between the generated candidates and uses a fast density computation. If we compare the average time for the Hruda et al. method of 1188.45 ms and the average time our method of 801.18 ms, we can state that our method is on average 1.48 times faster.

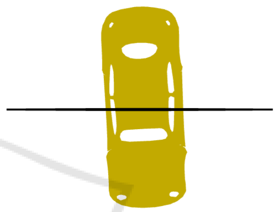

Figure 3: Result for the Beetle model if $t_a = 0.4$ is used.

10 CONCLUSION

The described method successfully finds the approximate symmetry planes in point clouds, and works well for various types of models. In terms of the relative symmetry measure the resulting planes are weaker symmetries than those of the Hruda et al. method, but the results are visually similar, see Figure 2, and our density based method is on average 1.48 times faster.

In the future, we aim to generalize the candidate creation process, and modify the method to detect different types of symmetries. We would also like to extend the method so it can work with different types of input, such as volumetric data, and exploit the detected planes for data compression. The algorithm could be further accelerated by computation of weights w_i on the GPU.

ACKNOWLEDGMENTS

This work was supported by the project 23-04622L, Data compression paradigm based on omitting self-evident information - COMPROMISE, of the Czech

Table 1: Measured results of our density based method and the Hruda et al. method (Hruda et al., 2021).

Input		Density peak method					Hruda et al. method	
Name	Number of points	t_a	D	s_{cell}	sym_{rel}	Time [ms]	sym_{rel}	Time [ms]
Ant	3495	0.4	25	0.1	0.8606616	**820**	0.9106182	1076
Armadillo	172974	0.5	50	0.05	0.5710908	**1266**	0.6171123	1680
Beetle	988	0.6	25	0.1	0.9107133	**611**	0.926909	856
Buddha	543103	0.6	25	0.08	0.4112466	**1012**	0.5553252	1186
Bunny	34834	0.4	25	0.05	0.4153833	1185	0.4667871	**1115**
Cow	2903	0.4	25	0.1	0.9133395	**659**	0.9134644	925
Elephant	19753	0.5	25	0.1	0.5669933	**679**	0.7926888	1032
Lucy	750001	0.6	25	0.05	0.4501815	**1439**	0.5110494	1877
Component1	1506	0.8	25	0.1	0.9787157	**123**	0.9789074	988
Component2	4302	0.8	25	0.1	0.9425972	**913**	0.9523025	1432
Component3	1410	0.8	25	0.1	0.7442631	**106**	0.7974733	906

Science Foundation, and by the Ministry of Education, Youth and Sports under the Students Research project SGS-2022-015.

REFERENCES

Cicconet, M., Hildebrand, D. G., and Elliott, H. (2017). Finding mirror symmetry via registration and optimal symmetric pairwise assignment of curves. *2017 IEEE International Conference on Computer Vision Workshops (ICCVW)*.

Ecins, A., Fermuller, C., and Aloimonos, Y. (2017). Detecting reflectional symmetries in 3d data through symmetrical fitting. *2017 IEEE International Conference on Computer Vision Workshops (ICCVW)*, page 1779–1783.

Fang, R., Godil, A., Li, X., and Wagan, A. (2008). A new shape benchmark for 3d object retrieval. *Lecture Notes in Computer Science*, page 381–392.

Gao, L., Zhang, L.-X., Meng, H.-Y., Ren, Y.-H., Lai, Y.-K., and Kobbelt, L. (2021). Prs-net: Planar reflective symmetry detection net for 3d models. *IEEE Transactions on Visualization and Computer Graphics*, 27(6):3007–3018.

Gothandaraman, R., Jha, R., and Muthuswamy, S. (2020). Reflectional and rotational symmetry detection of cad models based on point cloud processing. *2020 IEEE 4th Conference on Information & Communication Technology (CICT)*, 34:1–5.

Hruda, L., Dvořák, J., and Váša, L. (2019). On evaluating consensus in ransac surface registration. *Computer Graphics Forum*, 38(5):175–186.

Hruda, L., Kolingerová, I., and Váša, L. (2021). Robust, fast and flexible symmetry plane detection based on differentiable symmetry measure. *The Visual Computer*, 38(2):555–571.

Jacobson, A. (2024). Common 3d test models.

Ji, P. and Liu, X. (2019). A fast and efficient 3d reflection symmetry detector based on neural networks. *Multimedia Tools and Applications*, 78(24):35471–35492.

Kovács, E. (2012). Rotation about an arbitrary axis and reflection through an arbitrary plane. In *Annales Mathematicae et Informaticae*, pages 175–186.

Levoy, M., Gerth, J., Curless, B., and Pull, K. (2005). The stanford 3d scanning repository.

Li, B., Johan, H., Ye, Y., and Lu, Y. (2016). Efficient 3d reflection symmetry detection: A view-based approach. *Graphical Models*, 83:2–14.

Martinet, A., Soler, C., Holzschuch, N., and Sillion, F. X. (2006). Accurate detection of symmetries in 3d shapes. *ACM Transactions on Graphics*, 25(2):439–464.

Mitra, N. J., Guibas, L. J., and Pauly, M. (2006). Partial and approximate symmetry detection for 3d geometry. *ACM SIGGRAPH 2006 Papers on - SIGGRAPH '06*, page 560.

Mitra, N. J., Pauly, M., Wand, M., and Ceylan, D. (2013). Symmetry in 3d geometry: Extraction and applications. *Computer Graphics Forum*, 32(6):1–23.

Nagar, R. and Raman, S. (2019). Detecting approximate reflection symmetry in a point set using optimization on manifold. *IEEE Transactions on Signal Processing*, 67(6):1582–1595.

Shilane, P., Min, P., Kazhdan, M., and Funkhouser, T. (2004). The princeton shape benchmark. *Proceedings Shape Modeling Applications, 2004.*, page 167–388.

Wendland, H. (1995). Piecewise polynomial, positive definite and compactly supported radial functions of minimal degree. *Advances in Computational Mathematics*, page 389–396.

Yianilos, P. N. (1993). Data structures and algorithms for nearest neighbor search in general metric spaces. In *Proceedings of the Fourth Annual ACM-SIAM Symposium on Discrete Algorithms*, SODA '93, page 311–321, USA. Society for Industrial and Applied Mathematics.